PHYSICAL REVIEW B VOLUME 32, NUMBER 8 15 OCTOBER 1985

# $L_{2,3}$ absorption spectra of the lighter $3d$ transition metals

J. Zaanen and G. A. Sawatzky
*The Physical Chemistry Department of the Material Science Center, Nijenborgh 16, 9747 AG Groningen, The Netherlands*

J. Fink
*Kernforschungszentrum Karlsruhe, Institut für Nukleare Festkörperphysik, Postfach 3640, D-7500 Karlsruhe, Federal Republic of Germany*

W. Speier
*Institut für Festkörperforschung, Kernforschungsanlage Jülich, Postfach 1913, D-5170 Jülich, Federal Republic of Germany*

J. C. Fuggle
*Fysische Chemie, Faculteit der Wetenschappen, Katholieke Universiteit Nijmegen, 6525 ED Nijmegen, The Netherlands*
(Received 29 April 1985)

A theory is presented for the x-ray absorption spectra of materials characterized by bandwidths which are somewhat larger than the (quasiatomic) electron correlation energies. Assuming that an empty-band approximation is appropriate for nearly empty bands we show that the problem is much akin to the well-known Coulomb localization problem in Auger spectroscopy, with an enhanced sensitivity for exchange and multipole effects because of the dipole selection rules. Using first-principles band structure and atomic data as input for the theory, we calculate the spectra of Ca, Ti, and V and obtain good agreement with high-resolution experimental spectra.

## I. INTRODUCTION

In contrast to the heavier $3d$ transition metals the lighter $3d$ transition metals like Sc, Ti, V are, in their elemental form, considered to be well characterized by one-electron band theory because of relatively weak electron correlation effects. Strong indications for this are their nonmagnetic nature and the success of local-density band-structure calculations[1] in the interpretation of valence photoemission[2] and inverse photoemission experiments.[3] Because of the success of one-particle theories for these systems it is a surprise that they fail completely in describing the near-edge x-ray absorption spectra of lighter $3d$ transition metals.[4–7] In the preceding paper[7] we have presented detailed high-resolution near-edge data for the $2p \rightarrow 3d$ transitions of the $3d$ transition metals. We have noted that there are strong deviations from the expected local density-of-states picture. Inclusion of energy-dependent transition matrix elements[8] does not improve the situation much. The discrepancies observed are the following.

(1) A strong deviation from the statistical ratio of the $L_2$ to $L_3$ near-edge structure intensities.

(2) A line shape which deviates strongly from that expected from the density of states (DOS) above the Fermi level in that the near-edge intensity is suppressed and that further away from threshold it is enhanced relative to the DOS.

(3) A strong change in the apparent spin-orbit splitting, defined with respect to the $L_3$ and $L_2$ peak maxima, relative to that observed in $2p$ core-line photoemission.

In this paper we address these problems and show that they are all related to the same effect, namely, the atomic-like term splittings of a $2p^5 3d^1$ configuration. The dominant interaction responsible for the observed features is the $2p$-$3d$ exchange interaction. A strong interplay of the atomic exchange, spin-orbit, and solid-state band-structure effects causes the peculiar structures observed, which are intermediate between those expected for the free atom and those expected from the $d$-band density of states. It should be noted that the influence of exchange on optical spectroscopies is much more general than for the particular cases studied here. It has been used to explain the intensity ratios of excitons in ultraviolet optical spectroscopies of compounds,[9] the threshold singularity ratio in core-state optical absorption of Li metal,[10] the x-ray absorption spectra of rare-earth metals[11] and is present in the random-phase-approximation exchange scheme used to describe giant resonances as developed by Wendin.[12]

The paper is organized as follows. In Sec. II we review briefly the $L_{2,3}$ edge structure appearing in x-ray absorption spectroscopy for the free atom including also crystal-field effects. In Sec. III we show how the atom can be embedded in the solid and how band-structure effects can be included. Finally in Sec. IV we compare calculated line shapes to the experimental results of the preceding paper.

## II. THE ATOMIC $L_2$,$L_3$ XAS SPECTRA

In order to understand the physics involved in the line shapes found in solids, we first look at what would happen in an atom or ion like $Ca^{2+}$ with an empty $3d$ shell in

 

TABLE I. Results and fit parameters (in eV). The values of $F_0$ found for 20% reduction of $F_2$, $G_1$, and $G_3$ are tabulated. The values of $\Delta_{SO}$(expt.) and $\Delta_{SO}$(theor.) are measured from the maxima of the $L_3$ and $L_2$ structures.

| | $\delta E_f$ | $F_0$ $(2p\,3d)$ | $F_2$ $(2p\,3d)$ | $G_1$ $(2p\,3d)$ | $G_3$ $(2p\,3d)$ | $\Delta_{SO}$ (XPS) | $\Delta_{SO}$ (expt.) | $\Delta_{SO}$ (theor.) |
|---|---|---|---|---|---|---|---|---|
| Ca | 0.0 | 3.0 | 3.80 | 2.52 | 1.43 | 3.7 | 3.2 | 3.7 |
| Ti | 0.0 | 0.4 | 4.84 | 3.37 | 1.92 | 6.2 | 5.7 | 5.9 |
| V | 0.5 | 1.1 | 5.35 | 3.80 | 2.15 | 7.7 | 6.9 | 7.0 |

the ground state. This has been discussed to some extent previously by Barth *et al.*[6] who used the atomic results of Mansfield.[13]

The ground state of the atom is $^1S$ and therefore the only optically allowed transitions are to the $^1P$ final states. Considering only $2p$ to $3d$ transitions the electronic configuration of the final states is $p^5d^1$ which, in $LS$ coupling, split into the terms $^3F$, $^1F$, $^3D$, $^1D$, $^3P$, $^1P$ because of the $p$-$d$ Coulomb and exchange interactions. If spin-orbit coupling were negligible we would see only one line corresponding to the $^1P$ final state. Because of the large spin-orbit coupling of the $2p$ hole it is more appropriate to work in a $j$, $j$ representation. The transformation matrix from $LS$ to $jj$ coupling involving the $^1P$ state is given by[14]

$$\begin{array}{c} \\ (3/2,5/2) \\ (3/2,3/2) \\ (1/2,3/2) \end{array} \begin{array}{c} \begin{array}{ccc} ^3D_1 & ^3P_1 & ^1P_1 \end{array} \\ \begin{pmatrix} -\sqrt{3} & 3 & 3\sqrt{2} \\ 2\sqrt{3} & 4 & -\sqrt{2} \\ \sqrt{15} & -\sqrt{5} & \sqrt{10} \end{pmatrix} \end{array} \frac{1}{\sqrt{30}} \tag{1}$$

We see that we can expect to find a maximum of three lines which will reduce to two lines, $j_p=\frac{3}{2}$ and $j_p=\frac{1}{2}$, with an intensity ratio of 2:1 for negligible spin-orbit coupling of the $d$ electron and negligible $p$-$d$ Coulomb and exchange interactions.

Although the $d$-electron spin-orbit coupling is negligible, the Coulomb and exchange interactions are not. It is these interactions which cause a large redistribution of intensities and therefore strong deviations from a 2:1 intensity ratio. The Coulomb and exchange interactions are expressed in terms of the Slater integrals $F_2$, $G_1$, and $G_3$ for which calculated atomic Hartree-Fock values are used as given in Table I. In terms of the $j,j$ basis the interaction matrix elements are[14]

$$\underline{V}= \begin{array}{c} \begin{array}{ccc} (\frac{3}{2},\frac{5}{2}) & (\frac{3}{2},\frac{3}{2}) & (\frac{1}{2},\frac{3}{2}) \end{array} \\ \begin{pmatrix} -\frac{28}{175}F_2+\frac{12}{15}G_1 & -\frac{14}{175}F_2-\frac{4}{15}G_1 & -\frac{7\sqrt{5}}{175}F_2+\frac{4\sqrt{5}}{15}G_1 \\ -\frac{14}{175}F_2-\frac{4}{15}G_1 & -\frac{7}{175}F_2+\frac{4}{45}G_1 & \frac{14\sqrt{5}}{175}F_2-\frac{4\sqrt{5}}{45}G_1 \\ -\frac{7\sqrt{5}}{175}F_2+\frac{4\sqrt{5}}{15}G_1 & \frac{14\sqrt{5}}{175}F_2-\frac{4\sqrt{5}}{45}G_1 & \frac{20}{45}G_1 \end{pmatrix} \end{array} . \tag{2}$$

The eigenstates of the $p^5d^1$ final configuration are written as $|i\rangle=\alpha_i|3/2,5/2\rangle+\beta_i|3/2,3/2\rangle+\gamma_i|1/2,3/2\rangle$ and using Eq. (1) the optical spectrum is given by

$$\rho(\omega)=\sum_i \left|\frac{3}{\sqrt{2}}\alpha_i-\sqrt{2}\beta_i+\sqrt{10}\gamma_i\right|^2 \delta(\omega-E_i)\,, \tag{3}$$

where $E_i$ are the eigenvalues.

In Fig. 1(a) we show the calculated atomic spectrum of Ca taking $F_2=G_1=0$ and a $2p$ atomic spin-orbit splitting of 5 eV. The influence of Coulomb and exchange interactions is demonstrated in Fig. 1(b). In comparing this with Fig. 1(a) we see the large change in the ratio of the intensity of the $L_3$ peak to that of the $L_2$ peak, $I(L_3)/I(L_2)$, the shift to higher energy, and the apparent reduction in the spin-orbit splitting. The shift to higher energy (away from threshold) is interesting and is caused by the fact that the $^1P$ character of a $p^5d^1$ configuration always occurs at the high-energy side of the total multiplet structure.

The influence of the Coulomb and exchange interactions on the $I(L_3)/I(L_2)$ ratio is shown in Fig. 2. Here we used values of $F_2$ and $G_1$ for Ti and calculated the ratio of the intensity of the sum of the two lower energy lines to that of the highest energy line as a function of the spin-orbit splitting ($\Delta_{SO}$). Qualitatively this is the behavior seen in Fig. 1 of the previous paper. However, experimentally the statistical ratio of 2:1 is reached much more rapidly than the atomic calculation for the simple model final state ($p^5d^1$) predicts. This brings us to a problem which we will encounter in the solid-state calculation and which will limit the applicability of our theory to the lighter $3d$ transition metals. In the calculation we

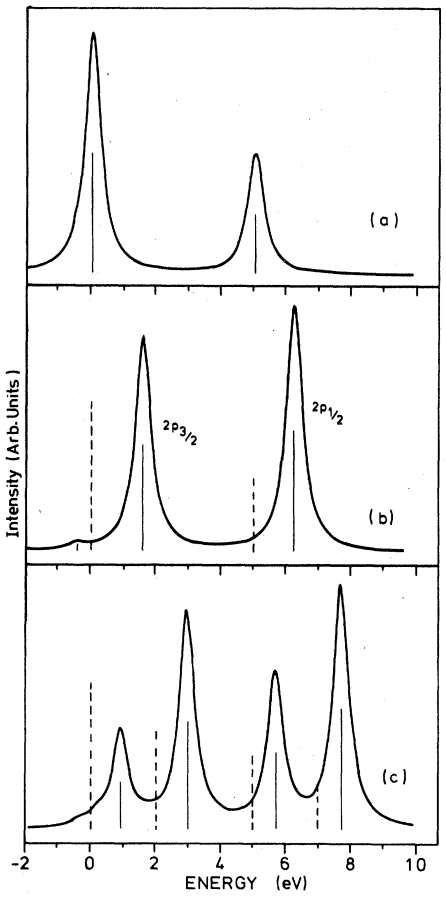


FIG. 1. Calculated atomic $2p^63d^0 \rightarrow 2p^53d^1$ absorption spectra ($\Delta_{SO}=5$ eV). In (a) and (b) results are shown for spherical symmetry. In (a) the Slater integrals are set to zero while in (b) we used the atomic Hartree-Fock values for the Slater integrals $F_2$ and $G_1$ of Ca. In (c) we show the atomic results for $O_h$ symmetry (10 $Dq=2$ eV). Solid lines include the Slater integrals and dashed lines correspond to the independent particle result.

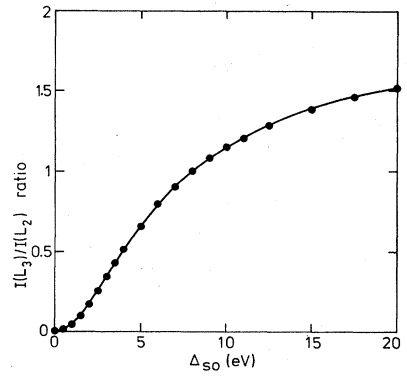


FIG. 2. Theoretical $I(L_3)/I(L_2)$ ratio as a function of the $2p$ spin-orbit splitting $\Delta_{SO}$ for a $2p^63d^0 \rightarrow 2p^53d^1$ atomic absorption using for the Slater integrals the Hartree-Fock values of Ti.

have neglected the possible presence of other $d$ electrons in the ground state. Although for the free atom this can easily be handled, it is by no means simple for the solid. There is, however, a qualitative argument which can be used. The dominant influence of $d$ electrons present in the ground state is to limit the amount of phase space available for the photon-excited $d$ electron. This in turn limits the amount of phase space available for the Coulomb and exchange interactions to be operative and therefore reduces their influence on the intensity ratios. An extreme example is an initial $d^9$ configuration where the final state is $p^5d^{10}$ with no phase space left for effects involving Coulomb and exchange interactions. The change in the $d$-band occupation as we go through the $3d$ series therefore causes the statistical limit to be reached much more rapidly than predicted by a $p^5d^1$ calculation.

Treating the other $d$ electrons as passive is only expected to be a valid approximation in the limit that the bandwidth is large compared to $d$-$d$ Coulomb or exchange interactions. In this case the number of $d$ electrons ($n$) on any given atom is fluctuating rapidly so that $n$ is not a constant of motion. For narrow-$d$-band materials like the ionic compounds the ground-state $d$ electrons cannot be treated as passive. In this case a full configuration interaction treatment is required for both the ground and excited states to describe the absorption spectra. Such a procedure is shown to be very successful for divalent Ni compounds.[15] The treatment of the intermediate-bandwidth case remains an open problem.

For the materials considered here the bandwidths ($\approx 6$ eV) are indeed much larger than the $d$-$d$ Coulomb interaction ($\approx 1$ eV) and also much larger than the $p$-$d$ interaction after screening by the extra $d$ electron in the final state. We therefore expect that at least for short times (in which the screening $d$ electron is still around the $p$ hole) the ground state $d$ electrons will not be strongly perturbed and can be treated as passive. Of course the details of the threshold behavior will involve long-time behavior in which the ground-state $d$ electrons also will play an important role.

Another problem we will encounter in the solid is the influence of crystal-field effects. The above calculation was done assuming spherical symmetry whereas the point group in the solid is often cubic. In a cubic point group the $d$ orbitals split into $t_{2g}$ and $e_g$ orbitals quenching the angular momentum. This, however, is quite easy to handle although the calculations become rather tedious because of the larger matrices involved. For the details we refer to similar calculations by Yamaguchi *et al.*[16] The influence of crystal fields is shown in Fig. 1(c) for Ca for an $O_h$ point group. The crystal-field splitting ($10Dq$) was taken to be 2 eV. We notice the appearance of extra splittings in the spectra. For the metals, however, we will show below that the effects of deviation from spherical symmetry are not large.

## III. THE SOLID STATE

Very qualitatively we see the same features in the solid-state $L_{2,3}$ electron energy-loss spectra (Fig. 2, previous paper) as those expected from the atomic calculation.

These features are the nonstatistical $I(L_3)/I(L_2)$ ratio, the shift of spectral weight *away* from threshold, and the reduction of the apparent spin-orbit coupling. However, in addition we also see features which can be related to structure in the $d$-band density of states. In fact, we know from band-structure calculations[1] and bremstrahlung isochromat spectroscopy (BIS)[3] that the $d$-band widths of lighter transition metals are 4—6 eV and therefore are larger but of the same order of magnitude as the splittings caused by the atomic $F_2$, $G_1$, and $G_3$ integrals. This means that band structure and atomic effects must be treated on an equal footing. In addition we have to deal with the problem of the influence of the monopole ($F_0$) $d$-$d$ Coulomb interaction. This is unimportant for the atom in which it merely shifts the spectrum as a whole and does not influence the spectral shape. In the solid, however, this attractive interaction is present only on the site containing the core hole, thereby breaking the translational symmetry and distorting the density of $d$ states. In fact, if large enough, this interaction causes a bound state to appear outside of the $d$ band giving rise to the "white line," frequently observed in XAS spectra, which is also referred to as a core-hole excitonic state. The influence of the attractive monopole $F_0$ interaction is to increase the spectral weight on the low-energy side of the $d$-band density of states. This is contrary to what is observed for Sc, Ti, V. However, we also concluded from our atomic calculation that the $F_2$ and $G_1$ integrals cause the optically accessible $^1P$ character to be shifted away from threshold. We are therefore dealing with competing processes which must both be included in the theory.

Another problem we must deal with is the screening of the Coulomb interactions in the solid state. A very general and understandable tendency is that the monopole $F_0$ integrals are strongly screened. This has been found for $3d$-$3d$ interactions and $3p$-$3d$ interactions in metals by Auger spectroscopy[17] and also for $2p$-$3d$ interactions in Ni (Ref. 18) and Ni impurities (Ref. 19). In fact for Sc, Ti, V we expect the $2p$-$3d$ $F_0$ to be reduced to a value close to zero in the metal. On the other hand, the higher multipole $F_2$ and exchange $G_1$, $G_3$ integrals are generally found to be only slightly reduced from the free-atom values.[17,19] This has very important consequences. In the free atom, $F_0$ is by far the dominant interaction, but in the solid it may in fact be smaller than $F_2$ and or $G_1$ because of screening. This kind of effect is observed in recent Auger spectra of $La_3Ni$ (Ref. 20) and also in Auger photoelectron coincidence spectra of Ni metal for the $d$-$d$ interactions[21] as well as in the apparent attractive Coulomb interactions observed in lighter-transition-metal Auger spectra.[22]

To describe the XAS spectra of the lighter $3d$ transition metals we will start with assuming that the $3d$ band is essentially empty in the ground state. The consequences of a partial filling of the $d$ bands will be discussed below. In the empty-band approximation the problem is reduced to that of two interacting particles in a solid. This is very similar to the Auger spectrum problem[23] except that we are now dealing with a localized core hole and a band electron instead of two band holes as in valence-valence Auger spectroscopy. The localized character of the core hole makes the present problem almost identical to that of the recently discussed impurity Auger spectrum.[24]

We assume that the $d$ bands can be represented in terms of a tight-binding model in which case the XAS spectrum is given by

$$\rho(\omega)=\frac{1}{\pi}\mathrm{Im}\sum_{j_1,j_2,j_1',j_2'} t(j_1j_2)G^{j_1'j_2'0}_{j_1j_20}(z)t(j_1'j_2') \tag{4}$$

with

$$J=j_1+j_2=j_1'+j_2'=1\ ,$$

$$z=\omega-i\epsilon\ ,$$

where $j_1$ and $j_2$ are the $j$ values for the $2p$ hole and $3d$ electron. $G^{j_1'j_2'0}_{j_1j_20}$ is the Green's function

$$G^{j_1'j_2'0}_{j_1j_20}(z)=\left\langle j_1j_20\left|\frac{1}{z-H}\right|j_1'j_2'0\right\rangle \tag{5}$$

with 0 labeling the site of the core hole. $t(j_1j_2)$ are the transition matrix elements which are simply proportional to the amount of $^1P$ character in the state $|j_1j_2\rangle$ as discussed for the free atom. The Hamiltonian $H$ includes, in addition to the free-atom Coulomb interaction ($F_0$,$F_2$), exchange interaction ($G_1$,$G_3$), and the spin-orbit splitting, also the $3d$ band structure ($\sum_{k,n}\epsilon_{kn}c^\dagger_{kn}c_{kn}$, $n$ is a band index).

Neglecting the effects of nonspherical symmetry the two-particle (electron-hole) Green's function defined in Eq. (5) can in analogy to the impurity Auger problem[24] be written as

$$G^{j_1'j_2'0}_{j_1j_20}(z)=g^{j_1j_20}_{j_1j_20}(z)\delta_{j_1j_1'}\delta_{j_2j_2'} +g^{j_1j_20}_{j_1j_20}(z)\sum_{j_1'',j_2''}\langle j_1j_2\,|\,V\,|\,j_1''j_2''\rangle G^{j_1'j_2'0}_{j_1''j_2''0}(z)\ , \tag{6}$$

where

$$g^{j_1j_20}_{j_1j_20}=\sum_{\substack{k\\(k>k_F)}}\frac{1}{z-\epsilon_{kj_2}-\epsilon_{j_1}} \tag{7}$$

and the matrix elements of $V$ are given in Eq. (2) for the free atom for those states which contain $^1P$ and in addition we must include the diagonal term $F_0$. The two-particle Green's functions corresponding to $j_1+j_2=J=1$ are then determined by the matrix relation

$$\underline{G}=\underline{g}+\underline{g}\,\underline{V}\,\underline{G} \tag{8}$$

or

$$\underline{G}=\frac{\underline{g}}{1-\underline{V}\,\underline{g}}\ , \tag{9}$$

which since $\underline{g}$ is diagonal by choice of the basis set

$$(\underline{g}^{-1}-\underline{V})\underline{G}=\underline{1}\ , \tag{10}$$

knowing the band structure and all the interactions we

can from this relation determine all the elements of $\underline{G}$. Using Eqs. (1) and (4) we find for the XAS spectrum

$$\rho(\omega)=\mathrm{Im}[\,18G^{3/2,5/2,0}_{3/2,5/2,0}(z)-12G^{3/2,3/2,0}_{3/2,5/2,0}(z)+2G^{3/2,3/2,0}_{3/2,3/2,0}(z)+6\sqrt{20}G^{1/2,3/2,0}_{3/2,5/2,0}(z)-2\sqrt{20}G^{1/2,3/2,0}_{3/2,3/2,0}(z)+10G^{1/2,3/2,0}_{1/2,3/2,0}(z)]\,. \quad (11)$$

In relation (7) the imaginary part of $g$ is the $d$-band partial density of states shifted by the $2p$ core-hole energy and the real part is its Hilbert transform.

To demonstrate the influence of the various contributions we did a calculation of the XAS line shape for a Gaussian $d$-band density of states [full width at half maximum (FWHM) 3 eV] and a $2p$ spin-orbit splitting of 5 eV. For $F_0=F_2=G_1=0$ we calculate the spectrum of Fig. 3(a) showing the original density of states as expected for a one-particle model and the statistical 2:1 $I(L_3)/I(L_2)$ ratio. In Fig. 3(b) is the spectrum obtained for $F_0=1$ eV and $F_2=G_1=0$ showing the previously mentioned effect of the shifting of intensity towards threshold. In Fig. 3(c) we show the spectrum for $F_0=0$ eV, $F_2=3.8$ eV, $G_1=2.52$ eV as calculated for Ca. We see the shift of spectral weight away from threshold and a strong enhancement of the $L_2$ intensity. As mentioned before, this shift and intensity change is due to the fact that only the $^1P$ character is probed by XAS which is shifted away from threshold due to $F_2$ and $G_1$.

Up to here we have assumed that the crystal symmetry is of no importance. Also this can be treated properly although the calculations become tedious because the matrix equations determining $\underline{G}$ [Eq. (10)] can become quite large. For example, in the cubic $O_h$ point group the representation in which $g$ [Eq. (7)] is diagonal is the $|j_1 t_{2g}\rangle$, $|j_1 e_g\rangle$ representation. We then also must write the interaction ($\underline{V}$) matrix in this representation after which Eq. (10) can be used. However, now we require the local symmetry-projected ($t_{2g}$ and $e_g$) density of states to determine $\underline{g}$ completely.

To show the influence of crystal symmetry we have used a model density of states represented by two Lorentzians, one for the $t_{2g}$ partial density of states and another of $\frac{2}{3}$ the intensity representing the $e_g$ projected density of states. The splitting was taken to be $10Dq=2$ eV and the widths were 1 eV.

In Fig. 4(a) we show the spectrum expected in one particle theory for $F_0=F_2=G_1=G_3=0$ which simply shows the original density of states. In Fig. 4(b) we have taken $F_0=0$ eV, $F_2=3.8$ eV, $G_1=2.52$ eV, and $G_3=1.43$ eV for Ca taking the cubic symmetry into account. In Fig. 4(c) the spectrum is calculated neglecting the cubic symmetry by merely using Eq. (10) and a $d$-band total density of states composed of the same two Lorentzians. Comparison of Fig. 3(c) with Fig. 3(b) shows that the spectrum is quite insensitive to differences in the $t_{2g}$ and $e_g$ density of states although if $10Dq$ were much larger than the free-atom term splittings or the partial bandwidths it would certainly be noticeable, as demonstrated for the free atom in Fig. 1(c).

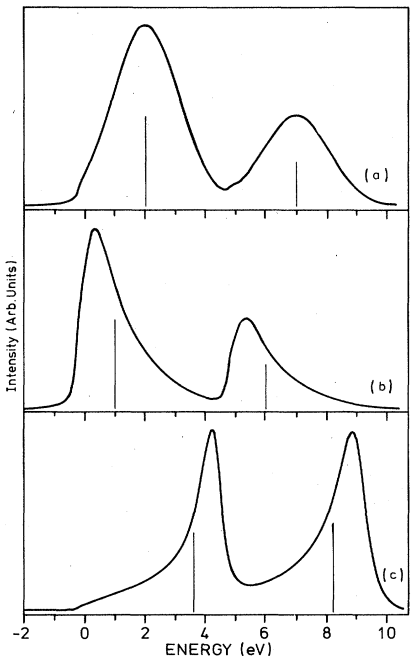


FIG. 3. Calculated solid-state $2p$ absorption spectra using Gaussian $d$-band density of states (FWHM of 3 eV) and a $2p$ spin-orbit splitting of 5 eV. In (a) we show the independent particle result. In (b) the effect of $F_0=1$ eV is shown while in (c) the influence of exchange and multiple Slater integrals ($F_2, G_1$) is shown, taking atomic Hartree-Fock values as calculated for Ca.

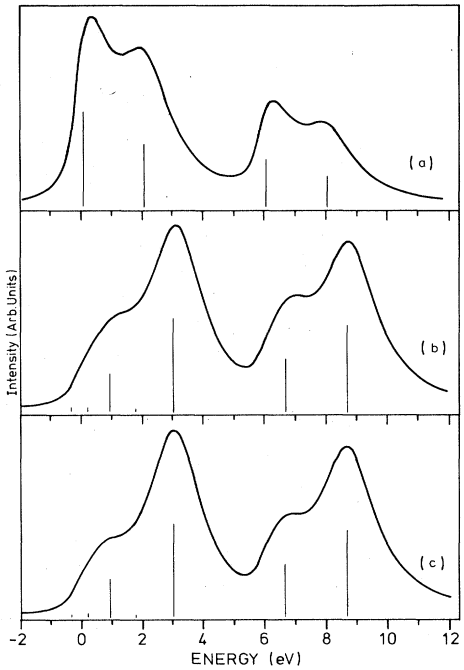


FIG. 4. Effect of lowered symmetry on solid-state absorption spectra. In (a) we show the independent particle spectrum using a density of states composed of two Lorentzians split by 2 eV. In (b) and (c) the exchange and multipole Slater integrals are included as in Fig. 3. In (b) the upper Lorentzian was identified with the $e_g$ and the lower with the $t_{2g}$ density of states ($O_h$ symmetry). In (c) the same double-Lorentzian density of states was used for $t_{2g}$ and $e_g$.

## IV. RESULTS AND DISCUSSION

In this section we use the theory described in the previous sections to calculate the XAS and electron-energy-loss (EELS) spectra of the lighter $3d$ transition metals. The $F_2$, $G_1$, and $G_3$ $2p$-$3d$ Coulomb integrals were determined using an atomic Hartree-Fock program[25] and these values are tabulated in Table I for Ca, Sc, Ti, V. Generally it is found that Hartree-Fock theory overestimates these interactions for the free atom by about 10% because of atomic correlation effects. Screening in the solid may reduce these by a further 10—20%. The $2p$ spin-orbit splitting was taken from x-ray photoemission results.[26] The $F_0$ Coulomb integrals will be treated as parameters because of the large uncertainty in the screening contribution.

The remaining unknown is the band structure. For Ca (fcc) and V (bcc) we used Koringa-Kohn-Rostoker band structure results[27] for the $d$-band partial density of states. Also the $t_{2g}$ and $e_g$ symmetry-projected partial density of states were determined and these are shown in Figs. 5(a) and 5(c). For Ti (hcp) the $d$-band density of states [Fig. 5(b)] was derived from linearized augmented-plane-wave calculations of Müller.[28] Because of the hcp structure the symmetry projection was not possible. Recent bremsstrahlung isochromat spectroscopy (BIS) measurements are in good agreement with the band-structure calculations. The only discrepancy of importance concerns the location of the Fermi level relative to structure in the $d$-band density of states for V. Good agreement with BIS can be obtained by shifting the Fermi level somewhat. The shifts we used can be found in Table I ($\delta E_F$).

In Fig. 6(a) we have reproduced the experimental EELS $L_{2,3}$ edge structure of V. As mentioned in the preceding paper[7] the thresholds are fixed by the XPS core line-binding energies. Figure 6(b) is the spectrum expected using a single-particle theory which corresponds to the $d$-band density of states. Figure 6(d) is the calculated spectrum using the theory of Sec. III with $F_0=1.1$ eV and $F_2$, $G_1$, and $G_3$ reduced by 20% from the free-atom values. The theory very nicely shows the shift of spectral weight away from threshold for the $L_3$ edge and to a lesser extent for the $L_2$ edge. Also the increase in the $L_2$ intensity and the apparent decrease in the spin-orbit splitting are well described as compared to one-particle theory. For comparison we show in Fig. 6(c) the calculated spectrum for $F_0=0.9$ eV and a 30% reduction of the other Coulomb and exchange integrals. Note that a decrease in $F_0$ must be accompanied by a corresponding decrease in $F_2$ and $G_1$ to get the peak positions right. This effect was discussed in Sec. II. A discrepancy remaining is the detailed line shape which we discuss below.

V is a quite simple example because as seen from Fig. 4 the unoccupied $d$ density of states corresponds to a single broad peak. Ti, on the other hand, shows a double-peaked structure and we might expect a more complicated line shape. In Fig. 7(a) the experimental spectrum of Ti is reproduced which again deviates strongly from the one-particle theory shown in Fig. 7(b). As for V good agreement is obtained using our theory as shown in Figs. 7(c)

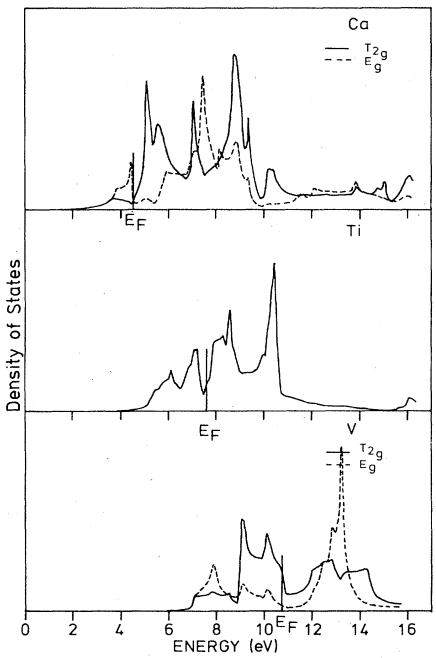


FIG. 5. Calculated $d$ density of states for Ca, Ti, and V. For Ti the total $d$ density of states is shown while for Ca and V the decomposition in the $t_{2g}$ and $e_g$ partial density of states is shown.

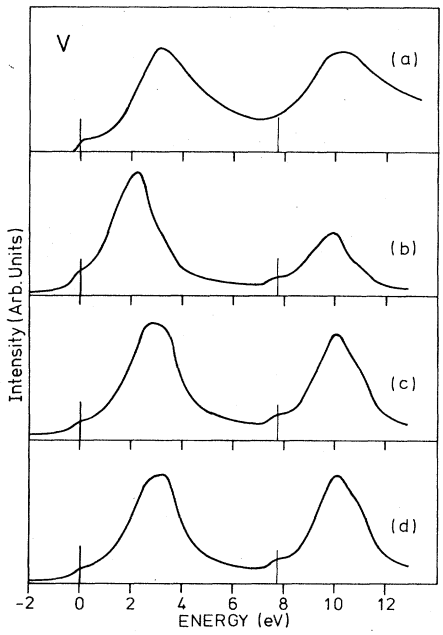


FIG. 6. Results for V. (a) The experimental $L_{2,3}$ spectrum of Fink *et al.* (Ref. 7). (b) The independent particle result neglecting matrix elements and transitions to $s$ states. (c) and (d) including two-particle correlation effects, using as parameters, respectively, $F_0=0.9$ eV, $F_2$, $G_1$, $G_3$ reduced by 30% and $F_0=1.1$ and 20% reduction of $F_2$, $G_1$, $G_3$ from their atomic Hartree-Fock values. In spectra (b)—(d) an energy independent lifetime broadening of 0.6 eV (FWHM) was assumed.

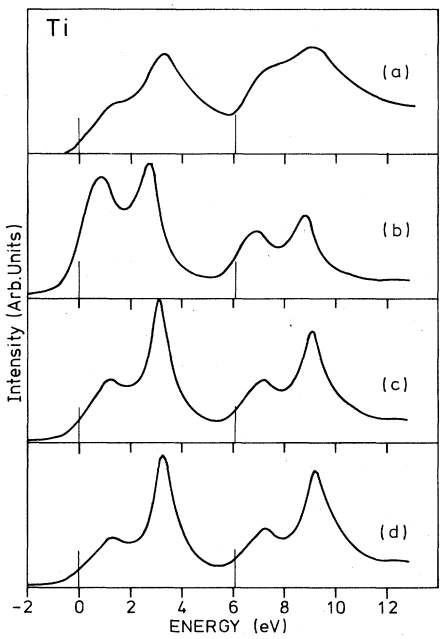


FIG. 7. Results for Ti. (a) The experimental spectrum. (b) The one-particle results. (c) and (d): The results of a two-particle calculation using parameters, respectively, $F_0=0.3$ eV and $F_2$, $G_1$ reduced by 40% and $F_0=0.3$ eV and $F_2$, $G_1$ reduced by 20%.

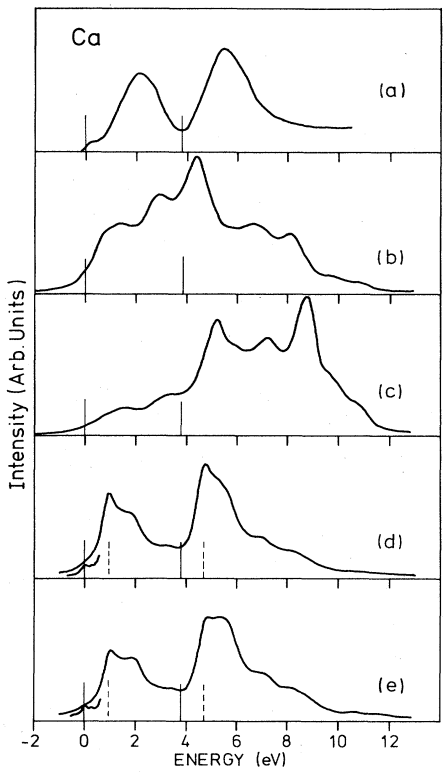


FIG. 8. Results for Ca. (a) The experimental spectrum. (b) The independent particle result. (c) Taking only into account the $F_2$, $G_1$, and $G_3$ integrals. (d) and (e): The $F_2$, $G_1$, and $G_3$ integrals reduced by, respectively, 30% and 20% and, in both pictures, $F_0=3$ eV. The dashed lines indicate the position of the single-particle threshold. The presence of a bound state at threshold is shown in (d) and (e) as obtained by reducing the broadening to 0.2 eV (FWHM).

and 7(d) obtained for $F_0=0.3$ and a 40% reduction of $F_2$ and $G_1$ and 7(d) obtained for $F_0=0.3$ and a 40% reduction of $F_2$ and $G_1$ and $F_0=0.4$ eV and a 30% reduction of $F_2$ and $G_1$, respectively. The theory predicts the shift of spectral weight away from threshold, the increase in $L_2$ intensity and a decrease in the apparent spin-orbit splitting. The discrepancies in the details of the line shapes are also primarily in the widths. We expect that very much the same picture can be obtained for Sc metal which we did not calculate.

The final example is Ca for which the $3d$ band is essentially empty initially. The discrepancy between experiment [Fig. 8(a)] and one-particle theory [Fig. 8(b)] is larger than in any other sample used. Furthermore, the discrepancy is also different in that here the spectral weight is shifted towards threshold rather than away from it. As discussed in Sec. III this can happen if the effect of $F_0$ is larger than that of $F_2$ and $G_1$. In Fig. 8(c) is a calculated spectrum, for $F_0=0$ and $F_2$ and $G_1$ reduced by 20% from the free-atom value, showing the shift of spectral weight in the opposite direction to that measured. We conclude that $F_0$ in Ca must be abnormally large as compared to that in Ti, V, which would be the case if the screening were much less efficient. Also in core photoemission anomalous behavior of Ca metal is found. The $2p$ photoemission lines of Ca are accompanied by a large satellite.[29] More direct evidence for a charge-transfer-like screening mechanism has been found by Fujimori *et al.*[30] who found a close resemblance between the shape of the $3p$ photoemission and the calculated $3p^5 3d^1$ multiplet structure. This suggests the formation of a $3d$-bound state in the core-hole potential which is also consistent with the appearance of satellite structure.[31]

Although in the above theory there will always be a bound state beneath the one-electron threshold of the absorption due to the presence of the sharp Fermi-level cutoff, closer examination shows that this state is less than 0.1 eV from the one electron threshold in the Ti and V spectra.[32] Due to the large $F_0$ interaction in Ca, on the other hand, a bound state appears at approximately 1 eV below the one-electron threshold as indicated in Figs. 8(d) and 8(e). The interpretation of Fujimori *et al.*[30] is confirmed at least qualitatively by these absorption results. In Figs. 8(d) and 8(e) we show the calculated spectra for $F_0=3$ eV and $F_2$, $G_1$ reduced by 30% and 20% respectively, from the free-atom values. We see that these results are in good agreement with experiment.

In Table I we have listed the values of the apparent spin-orbit splitting and $F_0$ as found from the theory. There is an interesting variation in $F_0$ which deserves comment. As mentioned above, $F_0$ is strongly screened in the solid. However, the screening is expected to depend on the density of states at the Fermi level. For example, a sudden decrease in $F_0(dd)$ is found from Auger spectroscopy[21] on going from Cu to Ni corresponding to the large

increase in the density of states at the Fermi level. The density of states in the vicinity of the Fermi level decreases on going from Ti to V to Ca. We note that the $F_0$ values follow the changes in the density of states at the Fermi level.

As mentioned above, there still are discrepancies remaining between theory and experiment. The most obvious is the failure to describe the line shape in detail. In Figs. 5—7 we broadened the theoretical spectra with a 0.6-eV (FWHM) Lorentzian to simulate the lifetime of the core hole plus the experimental resolution, which is an estimate for the average width in the $L_3$ spectrum. We note that this overestimates the broadening at threshold but underestimates the broadening further away from the $L_3$ threshold. The additional broadening of the $L_2$ region can be explained by a Coster-Kronig decay channel. The additional overall broadening relative to the edge structure could have several explanations. First, we have neglected transitions into the $s$ band which in itself would contribute a rising background as observed experimentally. Also, however, the $3d$ states are hybridized with the $s$ band so that Fano-like interference effects could be present. In principle, this could be taken into account in the theory.

In addition, the line shape will be influenced by the presence of other $d$ electrons in the ground state. In our approach we have neglected these. The fact that the two-particle theory works so well is evidence that the ground-state valence electrons play a minor role in the XAS spectra, at least if the $d$ electron density is small compared to the degeneracy of the band. It is well known that the presence of ground-state conduction electrons can cause drastic effects on the core-line XPS spectra resulting in satellite structures and threshold singularities.[18,31] This is, at first glance, also expected for XAS spectra. However, there is a distinct difference between x-ray photoemission spectroscopy (XPS) and XAS which can best be understood by looking at the time development of the excitation. In XPS one suddenly switches on a core-hole potential at $t=0$ which can result in several lines corresponding to whether or not sufficient screening electrons were present at that site at time $t=0$. In XAS, however, one can choose the core-hole state so that a transition is made directly into the screening state at $t=0$ like a $p$-$d$ transition in transition metals. The remaining ground-state electrons, then, see only a small sudden change in potential so the presence of these electrons is much less important in describing the short time scale (high energy scale) properties.

We have now established that provided the density of $d$ electrons in the ground state is small we expect no large deviations due to their presence. However, these many-body effects can still affect the details of the line shape.

## V. CONCLUSIONS

We have presented a two-particle theory for describing XAS (ELS) line shapes which treats fully the atomic Coulomb and exchange interactions as well as the solid-state band-structure effects. The theory is extremely successful in describing the $L_3$ and $L_2$ edge structures explaining satisfactorily the shifts as compared to XPS, the change in apparent spin-orbit splitting, the $I(L_3)/I(L_2)$ ratio, as well as the large deviations from one-particle density-of-states calculations.

We find that the monopole ($F_0$)$2p$-$3d$ Coulomb interaction is strongly screened in the solid and that the screening is directly related to the $3d$ partial density of states at the Fermi level. The higher multipole ($F_2$) Coulomb and exchange ($G_1$,$G_3$) interactions are reduced by only 20—30% from the free-atom values. The efficient screening of $F_0$ causes the rather interesting effect that the higher multipole interactions dominate.

## ACKNOWLEDGMENTS

We thank J. E. Müller and R. Zeller for the provision of unpublished band-structure results. We are also grateful to M. Campagna for his encouragement of this line of work. This investigation was supported in part by the Netherlands Foundation for Chemical Research (SON) with financial aid from the Netherlands Organization for the Advancement of Pure Research (ZWO).

[1]V. L. Moruzzi, J. F. Janak, and A. R. Williams, *Calculated Electronic Properties of Metals* (Pergamon, New York, 1978).

[2]L. Ley, O. B. Dabbonsi, S. P. Kowalczyk, F. R. McFeely, and D. A. Shirley, Phys. Rev. B **16**, 5372 (1977).

[3]W. Speier, J. C. Fuggle, R. Zeller, B. Ackermann, K. Szot, F. U. Hillebrecht, and M. Campagna, Phys. Rev. B **30**, 6921 (1984).

[4]J. L. Dehmer, A. F. Starace, U. Fano, J. Sugar, and J. W. Cooper, Phys. Rev. Lett. **26**, 1521 (1971); R. E. Dietz, E. G. McRae, Y. Yafet, and C. W. Caldwell, *ibid.* **33**, 1372 (1974); L. C. Davis and L. A. Feldkamp, Solid State Commun. **19**, 413 (1976).

[5]R. D. Leapman and L. A. Grunes, Phys. Rev. Lett. **45**, 397 (1980); L. A. Grunes, Phys. Rev. B **27**, 211 (1983); H. Nakamura, K. Ichikawa, Y. Watanabe, and K. Tsutsumsi, J. Phys. Soc. Jpn. **52**, 4014 (1983).

[6]J. Barth, F. Gerken, and C. Kunz, Phys. Rev. B **28**, 3608 (1983).

[7]J. Fink, Th. Müller-Heinzerling, B. Scheerer, W. Speier, F. U. Hillebrecht, J. C. Fuggle, J. Zaanen, and G. A. Sawatzky, preceding paper, Phys. Rev. B **32**, 4899 (1985).

[8]J. E. Müller, O. Jepsen, and J. W. Wilkins, Solid State Commun. **42**, 365 (1982); G. Materlik, J. E. Müller, and J. W. Wilkins, Phys. Rev. Lett. **50**, 267 (1983); J. E. Müller and J. W. Wilkins, Phys. Rev. B **29**, 4331 (1984); J. E. Müller, O. Jepsen, O. K. Andersen, and J. W. Wilkins, Phys. Rev. Lett. **40**, 720 (1978).

[9]Y. Onodera and Y. Toyozawa, J. Phys. Soc. Jpn. **22**, 833 (1967).

[10]Y. Onodera, J. Phys. Soc. Jpn. **39**, 1482 (1975).

[11]J. M. Esteva, R. C. Karnatak, J. C. Fuggle, and G. A. Sawatzky, Phys. Rev. Lett. **50**, 910 (1983); F. P. Netzer, G.

Strasser, and J. A. D. Matthew, *ibid.* **51**, 211 (1983).
[12]G. Wendin, Phys. Rev. Lett. **53**, 724 (1984).
[13]M. W. D. Mansfield, Proc. R. Soc. London, Ser. A **348**, 143 (1976).
[14]E. U. Condon and G. H. Shortley, *The Theory of Atomic Spectra* (Cambridge University, London, 1959).
[15]G. van der Laan, J. Zaanen, and G. A. Sawatzky (unpublished).
[16]T. Yamaguchi, S. Shibuya, S. Suga, and S. Shin, J. Phys. C **15**, 2641 (1982).
[17]E. Antonides, E. C. Janse, and G. A. Sawatzky, Phys. Rev. B **15**, 1669 (1977); **15**, 4596 (1977); M. Ohno and G. Wendin, J. Phys. B **12**, 1305 (1979); E. Antonides, Ph.D. thesis, University of Groningen, The Netherlands, 1977.
[18]L. A. Feldkamp and L. C. Davis, Phys. Rev. B **22**, 3644 (1980); L. C. Davis and L. A. Feldkamp, Solid State Commun. **34**, 141 (1980).
[19]A. Bosch, H. Feil, G. A. Sawatzky, and N. Martensson, Solid State Commun. **41**, 355 (1982).
[20]J. C. Fuggle, P. A. Bennett, F. U. Hillebrecht, A. Lenselink, and G. A. Sawatzky, Phys. Rev. Lett. **24**, 1787 (1983); P. A. Bennett, J. C. Fuggle, F. U. Hillebrecht, A. Lenselink, and G. A. Sawatzky, Phys. Rev. B **27**, 2194 (1983).
[21]H. W. Haak, J. Zaanen, and G. A. Sawatzky (unpublished); H. W. Haak, Ph.D. thesis, University of Groningen, 1983.
[22]D. K. G. de Boer, C. Haas, and G. A. Sawatzky, J. Phys. F **14**, 2769 (1984).
[23]G. A. Sawatzky, Phys. Rev. Lett. **39**, 504 (1977); M. Cini, Solid State Commun. **53**, 716 (1975).
[24]M. Vos, D. van der Marel, and G. A. Sawatzky, Phys. Rev. B **28**, 4315 (1983).
[25]R. D. Cowan, *The Theory of Atomic Structure and Spectra* (University of California, Berkeley, 1981).
[26]J. C. Fuggle and N. Martensson, J. Electron Spectrosc. Relat. Phenom. **21**, 275 (1980).
[27]R. Zeller (unpublished).
[28]J. E. Müller (unpublished).
[29]L. Ley, N. Martensson, and J. Azoulay, Phys. Rev. Lett. **45**, 1516 (1980).
[30]A. Fujimori, J. H. Weaver, and A. Franciosi, Phys. Rev. B **31**, 3549 (1985).
[31]A. Kotani and Y. Toyozawa, J. Phys. Soc. Jpn. **37**, 912 (1974).
[32]In Figs. 6 and 7 we took as a zero of energy the one-electron threshold energy. The pronounced tailing on the low-energy side of the theoretical spectra of the threshold is due to the convolution procedure we used to mimic lifetime effects which is certainly not appropriate. (Energy-dependent lifetime.)